A Facile Method for the Preparation of Gold Glyconanoparticles from Free Oligosaccharides and Their Applicability in Carbohydrate-Protein Interaction Studies

Koen M. Halkes,[a] Adriana Carvalho de Souza,[a] C. Elizabeth P. Maljaars,[a] Gerrit J. Gerwig,[a] and Johannis P. Kamerling*[a]

Dedicated to Professor András Lipták on the occasion of his 70th birthday

Keywords: Gold glyconanoparticles / Carbohydrates / Surface plasmon resonance / UV/Vis spectroscopy / Transmission electron microscopy

The weak binding affinity of monomeric oligosaccharides with carbohydrate-binding proteins are hampering their use in in-vivo and in-vitro bio-assays. Gold glyconanoparticles (GNPs), prepared from synthetic oligosaccharides, have been used to overcome this weak binding affinity. In this paper, a convenient method for the preparation of GNPs from free oligosaccharides is presented. The reductive amination of saccharides with trityl-protected cysteamine, followed by detritylation, afforded cysteamine-extended saccharides that could be used for the preparation of GNPs under reducing conditions in water. The robust chemistry and facile purification of intermediate and final compounds ensure high yields and reproducible results and the, subsequent, preparation of GNPs proceeded smoothly, even with minute quantities (nanomolar scale) of the cysteamine-extended saccharide. The described method was used to synthesize a series of *gluco*- and *manno*-oligosaccharide-containing GNPs. The prepared GNPs were validated in interaction studies with Con A, using either surface plasmon resonance (SPR), UV/Vis spectroscopy, or transmission electron microscopy (TEM). The described method for the preparation of water-soluble gold glyconanoparticles can be used for the identification of carbohydrate ligands for novel carbohydrate-binding proteins, and can find application as inhibitors of pathological interactions.

Introduction

Complex glycans that are attached to proteins and lipids coat all eukaryotic cells and are also found in the extracellular space between cells. They affect, through non-covalent interactions with other biomolecules, a great variety of biological processes ranging from development to cell-adhesion, and from signaling to infections by viral and bacterial agents.[1–4] Therefore, complex glycans represent a promising source for the development of new pharmaceutical agents. Before being able to tap the vast potential of complex glycans in drug development, fundamental challenges to clarify important structure-activity relationships have to be overcome. One of these challenges is the weak interaction of a carbohydrate in a 1:1 complex with its complementary biomolecule ($K_d \approx 10^{-3}$ M). To give these interactions biological relevance, Nature often presents carbohydrates multivalently or clustered on cell or tissue surfaces.[5]

The interest in designing multivalent or clustered carbohydrate analogues, that will mimic the natural cell or tissue surface and bind with high affinity to proteins, has been growing. Synthetic oligosaccharides, that are elongated with a suitable spacer, have been conjugated to carrier-proteins,[6] dendrimers,[7] and polystyrenes.[8] Recently, gold nanoparticles were coated with biologically relevant, synthetic saccharides.[9,10] The globular shape and the multivalent display of oligosaccharides at their surface make gold glyconanoparticles (GNPs) extremely suitable to overcome both the low binding affinity of monomeric oligosaccharides to carbohydrate-binding proteins[11,12] and the weak carbohydrate–carbohydrate self-recognition.[13,14] Complete water solubility, high storage stability, and no or low cytotoxic activity are some of the advantages associated with the use of GNPs in in-vitro and in-vivo bio-assays.

The synthesis of the thiol-spacer-containing oligosaccharides, necessary for the preparation of the above-mentioned GNPs, can be difficult and time-consuming. To further the use of GNPs in the field of glycobiology, simple methods for the preparation of GNPs from isolated glycans (e.g. from N-glycoproteins or polysaccharide fragments) has to

[a] Bijvoet Center, Department of Bio-Organic Chemistry, Utrecht University,
Padualaan 8, 3584 CH Utrecht, The Netherlands
E-mail: J.P.Kamerling@chem.uu.nl

  DOI: 10.1002/ejoc.200500256

be explored. Robust chemistry for the introduction of a thiol-containing spacer in free oligosaccharides, facile purification protocols of the thiol-spacer-containing oligosaccharides, and the reliable generation of stable and water-soluble GNPs are a few of the required characteristics for the method to become successful.

In the current paper, such a method for the facile preparation of GNPs on a small scale from free saccharides is described. The applicability of the approach is demonstrated by the generation of a wide range of *gluco*- and *manno*-oligosaccharide-containing GNPs and their use in SPR, UV/Vis, and TEM based interaction studies with the model lectin Concanavalin A.

Results and Discussion

Synthesis of Compounds 1–21

To synthesize GNPs from free oligosaccharides, a thiol-containing spacer has to be introduced at their reducing end. Reductive amination is a well-documented and robust chemical method to connect an aglycon to a glycan and was, therefore, used for the introduction of cysteamine into free saccharides. Prior to the reductive amination reaction, the thiol function in cysteamine was protected with a trityl group to avoid side reactions. The trityl-protecting group was chosen as it can be smoothly removed under mild

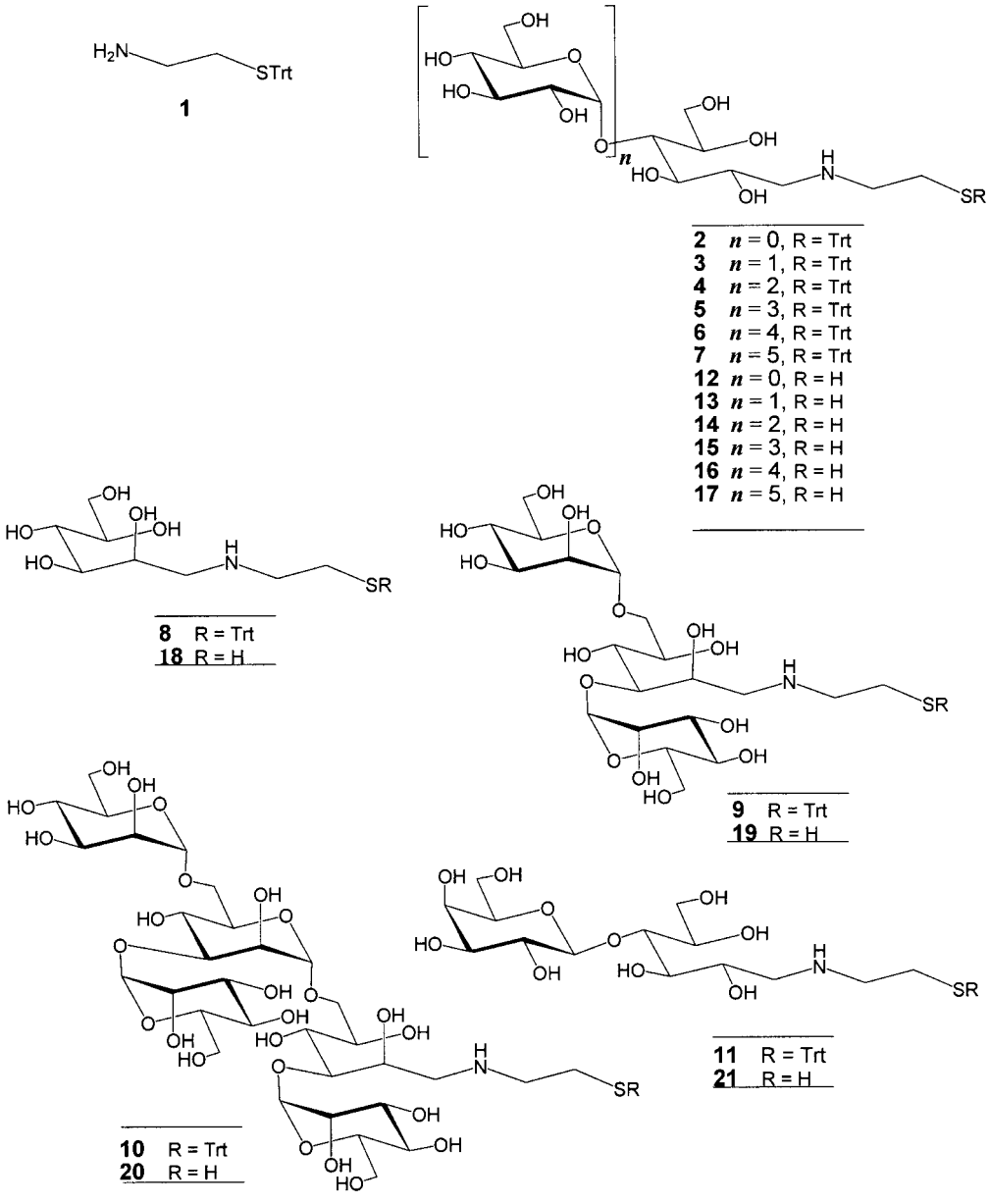

Figure 1. Synthesized thiol-spacer-containing saccharides.

acidic conditions and, additionally, its hydrophobic character facilitates the purification of the reaction products by RP-HPLC or in solid-phase extraction procedures. The hydrochloric acid salt of cysteamine was treated with trityl chloride in DMF to afford pure **1** (90% yield).

The free saccharide (glucose, maltose – maltohexaose, mannose, mannotriose, mannopentaose, or lactose) and **1** were dissolved in anhydrous, acidified dimethyl sulfoxide, and sodium cyanoborohydride was added. After heating at 65 °C for 2 h, followed by degradation of the reducing agent, dimethyl sulfoxide and unreacted saccharide were removed from the mixture by solid-phase extraction. Remaining **1** could be easily removed from the desired product by silica gel chromatography for the smaller saccharides (mono- to trisaccharide) or by either RP-HPLC or solution-phase extraction procedures for the larger oligosaccharides. The intermediates **2**–**11** (Figure 1) were, after characterization by high-resolution matrix-assisted laser desorption ionization time-of-flight (MALDI-TOF) mass spectrometry, directly used in the next reaction step. The trityl group was smoothly removed under acidic conditions, in the presence of a cation scavenger, to yield the pure products **12**–**21** (Figure 1) in good overall yields (61 to 85%), after solid-phase extraction. All products were characterized by high-resolution mass spectrometry and 1D and 2D NMR spectroscopy. It should be noted that the isolated products oxidized, over time, completely into their corresponding disulfide analogues, as seen by a downfield shift of approximately 0.25 ppm for the proton signals of the cysteamine residue.

Synthesis of Gold Glyconanoparticles

A modified literature procedure was used for the preparation of GNPs **Au-12** to **Au-21**.[15] Thus, an aqueous solution of thiol-spacer-containing saccharide **12** to **21** was added to an equimolar amount of aqueous tetrachloroauric acid, and incubated for 2 h with an excess of sodium borohydride. The generated GNPs were purified by centrifugal filtration. GNPs **Au-12** and **Au-18**, derived from glucose and mannose, respectively, were not completely stable, as judged by the minute amounts of precipitation formed after several cycles of lyophilization and redissolving in water. The GNPs **Au-13** to **Au-17** and **Au-19** to **Au-21**, that were derived from oligosaccharides, showed complete colloidal stability, even in buffers of elevated salt concentrations (HEPES buffer: 10 mM HEPES pH 7.4, 0.15 M NaCl). The various compounds were characterized by ^{1}H NMR, transmission electron microscopy (TEM), and monosaccharide composition analysis. The mean diameter, the percentage of carbohydrate, and the carbohydrate-surface coverage of GNPs **Au-13** to **Au-17** and **Au-19** to **Au-21** are shown in Table 1. Although the size and percentage of carbohydrate on the GNPs vary to some extent, the carbohydrate-surface coverage of the GNPs are in a narrow range (between 9 and 16%) when the thiol-spacer derivatized oligosaccharides are treated with tetrachloroauric acid in a 1:1 molar ratio.

As it is well known that reductive aminations can be easily performed with nanomolar amounts of starting oligosaccharides, it was investigated if GNPs could be prepared with this amount of cysteamine-extended oligosaccharides, thereby, making the method more attractive for the field of glycoscience. By replacing magnetic for ultrasonic stirring and using a more dilute $NaBH_4$ solution, it was possible to prepare stable GNPs from **17** and tetrachloroauric acid (1:3) on a 95 nmol scale (**Au-17a**, D_{core} = 2.46 ± 1.1 nm).

Application of GNPs Au-13 to Au-17 and Au-19 to Au-21 in Interaction Studies with Concanavalin A

To validate the usefulness of the prepared GNPs in various types of interaction studies, a binding study with the model lectin Concanavalin A (Con A) was initiated. Con A is a well-described lectin that binds α-D-mannose/α-D-glucose-containing glycans and, has long been recognized as an excellent system to study multivalent effects. The lectin is a tetramer above pH 7.0, and a dimer below pH 6.0. The carbohydrate-binding site in Con A is an extended groove on the surface of the protein, that can easily accommodate carbohydrates ranging from mono- to pentasaccharides, and is best suited to recognize the unique spatial arrangement of the trisaccharide α-D-Man*p*-(1→3)-[α-D-Man*p*-(1→6)]-D-Man.[18] Extrapolating from literature,[18] GNPs

Table 1. Physical characteristics of gold glyconanoparticles.

Glyconanoparticle	D_{core} (nm)	% CHO (carbohydrate)[16]	# gold atoms/ surface atoms[17]	# CHO molecules[a]/ % surface coverage
Au-13	3.38 ± 1.7	10%	1298/482	70/15%
Au-14a	1.99 ± 0.9	11%	314/174	32/12%
Au-14	2.16 ± 1.1	19%	309/162	25/16%
Au-14b	3.12 ± 1.8	10%	1133/436	64/15%
Au-15	2.00 ± 0.9	12%	314/174	77/12%
Au-16	2.79 ± 1.0	21%	807/348	47/13%
Au-17	1.79 ± 0.9	28%	314/174	23/13%
Au-19	3.84 ± 1.6	9%	2406/752	53/11%
Au-20	2.71 ± 1.1	16%	807/348	34/10%
Au-21	1.97 ± 0.8	9%	314/174	98/9%

[a] Calculated according to $n_{CHO} = [(n_{Au} \times MW_{Au}/100 - \%_{CHO}) \times \%_{CHO}]/MW_{CHO}$; where n_{CHO} is the number of sugar molecules on GNP, n_{Au} is the number of gold atoms in GNP.

Au-13 to **Au-17**, containing α-D-glucose ligands, can be classified as weak Con A binders, while the GNPs **Au-19** to **Au-20**, containing α-D-mannose ligands, constitute the strong Con A binders. In this paper, SPR, UV/Vis, and TEM studies of binding events between the model lectin Con A and the different GNPs are used as examples of their applicability in interaction studies.

SPR Studies: Con A was immobilized, as a dimer, on two channels of a CM5 sensor chip at 400 RU and 7,000 RU, respectively. Ethanolamine was immobilized on a third channel of the CM5 sensor chip, and served as the blank surface. Solutions of **Au-13** to **Au-17** and **Au-19** to **Au-21** (100 μg mL^{-1}) in HEPES buffer, containing 10 mM $CaCl_2$, were flown over the sensor chip. As expected, **Au-21**, displaying β-D-galactose residues on its surface, showed no binding on either of the Con A channels nor on the blank surface. On the sensor chip channel with 400 RU of Con A, only **Au-19** and **Au-20** showed a strong SPR binding signal (175 and 625 RU, respectively) while no detectable binding events with GNPs **Au-13** to **Au-17** could be observed. On the channel with 7,000 RU Con A, all *gluco*- and *manno*-oligosaccharide-containing GNPs showed strong SPR signals. An explanation of this finding can be ascribed to the affinity order for the carbohydrate-binding site of Con A: *manno*-oligosaccharides >> dextran polymers > *gluco*-oligosaccharides.[18] As dextran polymers form the matrix of CM5 sensor chips, competition reactions between the analytes and matrix polymers for the binding site of immobilized Con A have to be taken into consideration. As a consequence of the ligand affinity order of Con A, the mannose-containing GNPs (**Au-19** and **Au-20**) can efficiently compete for the carbohydrate-binding site of Con A leading to a SPR signal on both the 400 and 7,000 RU Con A channel. However, the *gluco*-oligosaccharide-containing GNPs will not be able to remove dextran from the carbohydrate-binding site of Con A. In the flow cell with 400 RU Con A, the chance that all the binding sites are occupied by dextran is high and, therefore, no SPR signal is observed when GNPs **Au-13** to **Au-17** are injected. Statistically, in the 7,000 RU Con A channel free carbohydrate-binding sites are present for binding with **Au-13** to **Au-17**.

In Figure 2 (parts a and b), the binding curves of the various GNPs, at a 100 μg mL^{-1} concentration, on the 7,000 RU Con A sensor surface are shown. The effect of the avidity on the SPR response is most clearly seen when parts a and b of Figure 2 (a: sensorgrams of weak Con A binders; b: sensorgrams of strong Con A binders) are compared. The strong interaction of the *manno*-oligosaccharide-presenting GNPs ensures that more material is collected on the sensor surface as compared to the *gluco*-oligosaccharide-presenting GNPs, thereby, leading to a stronger SPR response. Besides the avidity of the GNPs for Con A, also the size of the GNPs is reflected in the observed SPR response. To demonstrate this effect, GNPs **Au-14a** (D_{core} = 1.99 ± 0.9 nm), **Au-14** (D_{core} = 2.16 ± 1.1 nm), and **Au-14b** (D_{core} = 3.12 ± 1.8 nm) were prepared from **14** and tetrachloroauric acid, in different molar ratios (see Exp. Sect.). The sensorgrams of these GNPs are shown in part c of Figure 2. It

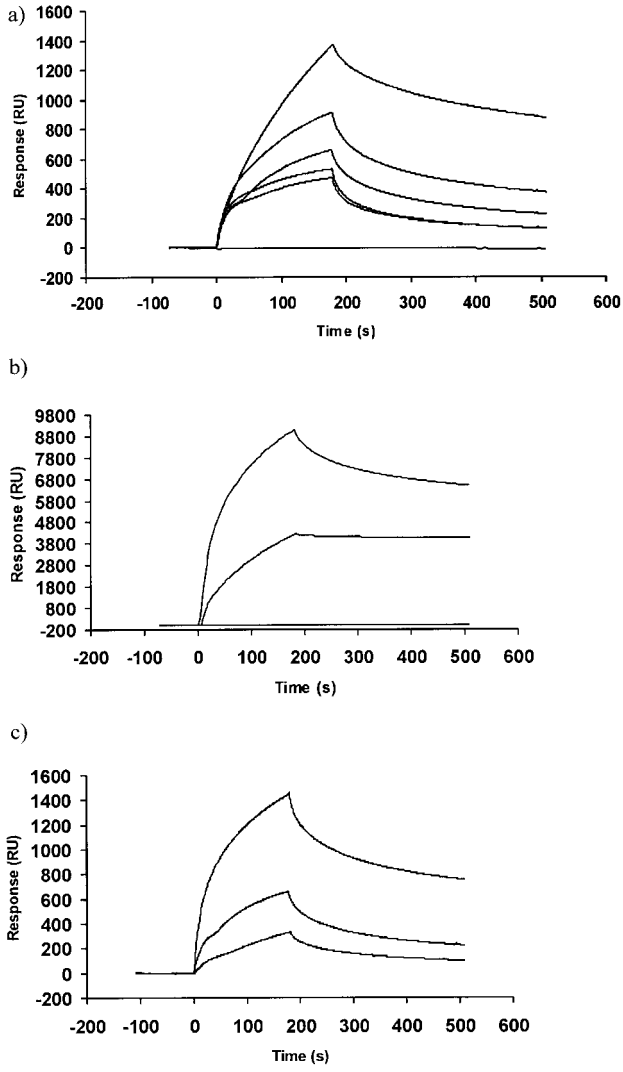

Figure 2. Biacore sensorgrams of the interactions between various GNPs (100 μg mL^{-1}) and Con A. a: Curves from top to bottom: **Au-13**, **Au-16**, **Au-14**, **Au-15**, **Au-17**, and **Au-21**. b: Curves from top to bottom: **Au-19**, **Au-20**, and **Au-21**. c: Curves from top to bottom: **Au-14b**, **Au-14**, and **Au-14a**.

is clearly visible that the largest particle gives rise to the highest SPR response.

The avidity of the GNPs for Con A can be, qualitatively, established from the dissociation phase of the binding curves. Dissociation can be clearly seen in the **Au-13** to **Au-17** series (Figure 2, part a), some dissociation can be observed for **Au-19**, and no or negligible dissociation is seen for **Au-20** (Figure 2, part b). Another qualitative indication for the avidity of the GNPs for the lectin is the method of regeneration of the sensor chip surface. Complete regeneration of the Con A surface that has been treated with **Au-13** to **Au-17** is achieved by injecting, for 5 min, 150 mM methyl α-D-mannopyranoside. Under the same regeneration conditions, approximately 30% of **Au-19** and none of the **Au-20** was removed from the sensor surface. More stringent regeneration conditions are required for the removal of **Au-19** and **Au-20** from the sensor surface (see Exp. Sect.).

To establish the minimum GNP concentration that could still be observed in SPR binding experiments, a dilution series of **Au-15** (Figure 3, part a) and **Au-19** (Figure 3, part b) was injected over the 7,000 RU Con A sensor surface. It is clear that even at the lowest concentrations tested (2.34 μg mL^{-1} and 0.26 μg mL^{-1} for **Au-15** and **Au-19**, respectively) a detectable SPR response could be seen (10 to 20 RU).

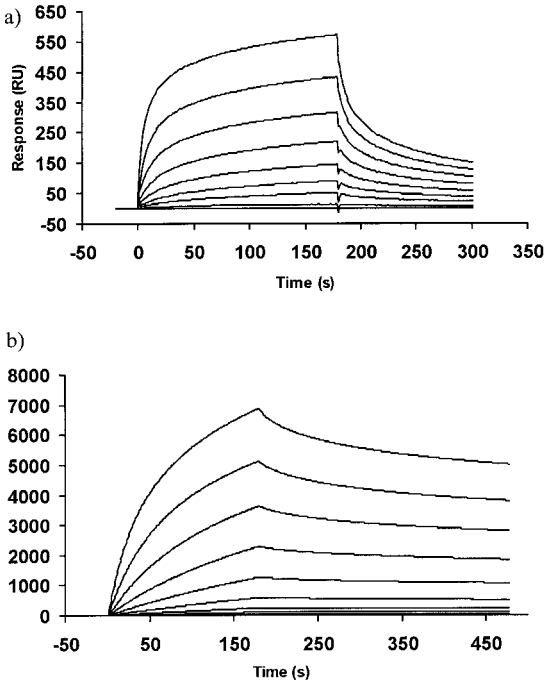

Figure 3. Composite sensorgrams of GNP concentration experiments with Con A. a: **Au-15** (concentration from top to bottom: 300, 150, 75, 37.5, 18.75, 9.38, 4.69, 2.34 μg mL^{-1}). b: **Au-19** (concentration from top to bottom: 66.67, 33.33, 16.67, 8.33, 4.16, 2.08, 1.04, 0.52, 0.26 μg mL^{-1}).

Finally, a competition experiment between **Au-17** (100 μg mL^{-1}; containing 0.028 mg intact maltopentaose) and maltopentaose (0.03–1.79 mg) was performed. The composite sensorgrams shown in Figure 4 illustrate that a large excess of free maltopentaose had to be used to obtain complete inhibition of binding between **Au-17** and Con A, thereby

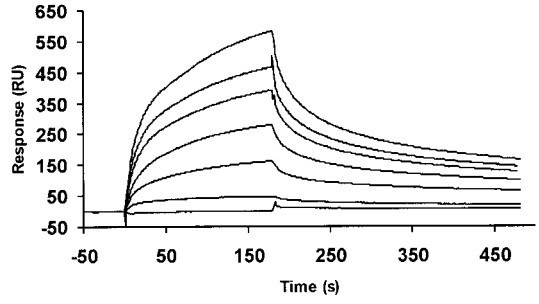

Figure 4. Composite sensorgrams of competition experiments between GNPs **Au-17** (100 μg mL^{-1} stock solution) and maltopentaose for the binding to Con A. To 100 μL of the **Au-17** stock solution were added increasing amounts of maltopentaose (from top to bottom: 0, 0.03, 0.06, 0.12, 0.24, 0.89, and 1.79 mg).

clearly demonstrating the multivalent binding character between the GNPs and Con A.

UV/Vis Studies: Previously, it has been shown[11] that lactose-containing GNPs (prepared starting from *p*-aminophenyl lactoside and PEGylated gold nanoparticles) exhibit selective aggregation when exposed to *Ricinus communis* agglutinin (RCA), a bivalent lectin specifically recognizing terminal β-D-galactose residues. During the aggregation of the GNPs with RCA, a broadening and red-shift in the particle surface plasmon band from 520 nm to a longer wavelength[19] was observed, leading to a loss of absorption at 520 nm. Recently, the same phenomenon was described for mannose-coated gold nanoparticles that were incubated with tetravalent Con A.[20] The loss of absorption at 520 nm[11] or the increase of absorption at 620 nm[20] could be followed by UV/Vis spectroscopy, and used in qualitative and quantitative bio-assays. Although the GNPs **Au-13** to **Au-17** and **Au-19** to **Au-21** are significantly smaller than the ones used above (8.9 nm[11] or 16 nm[20]), an absorption band near λ = 520 nm could be observed in all cases and used for monitoring aggregation events in an UV/Vis-spectrometer. Figure 5 shows the representative UV/Vis spectra of GNPs **Au-13** to **Au-17** and **Au-19** to **Au-21**, recorded for 6 h after addition of tetravalent Con A. With the exemption of **Au-21** (red line in Figure 5) that, as expected, showed no specific binding to Con A, all GNPs show the same pattern in the UV/Vis spectra: An initial increase in absorbance at 520 nm that is followed by a decrease in absorbance. The initial increase in absorbance is suggested to originate from the initial formation of small clusters (approximately 10 nm) of Con A-interlinked GNPs that may lead to a stronger surface plasmon band. Over the time, the cluster

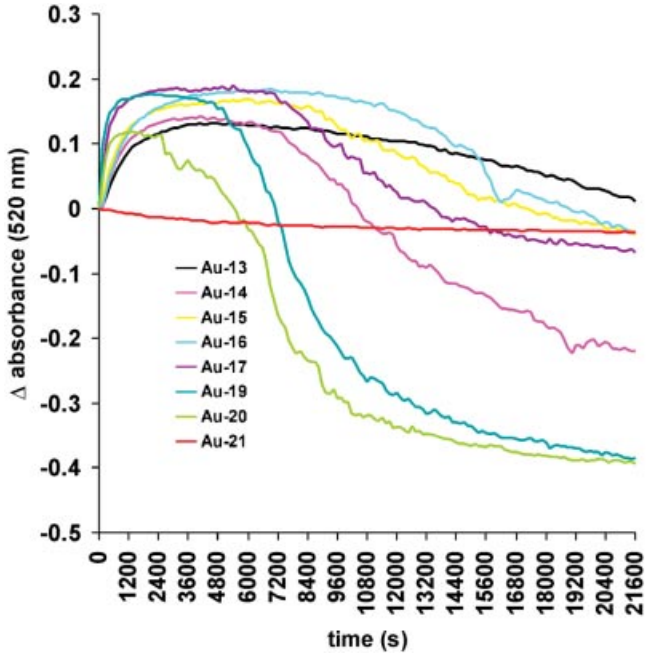

Figure 5. Composite UV/Vis spectra of the aggregation between different GNPs (50 μg) and Con A (50 μg) in 550 μL HEPES buffer, containing 10 mM $CaCl_2$ (pH 7.4).

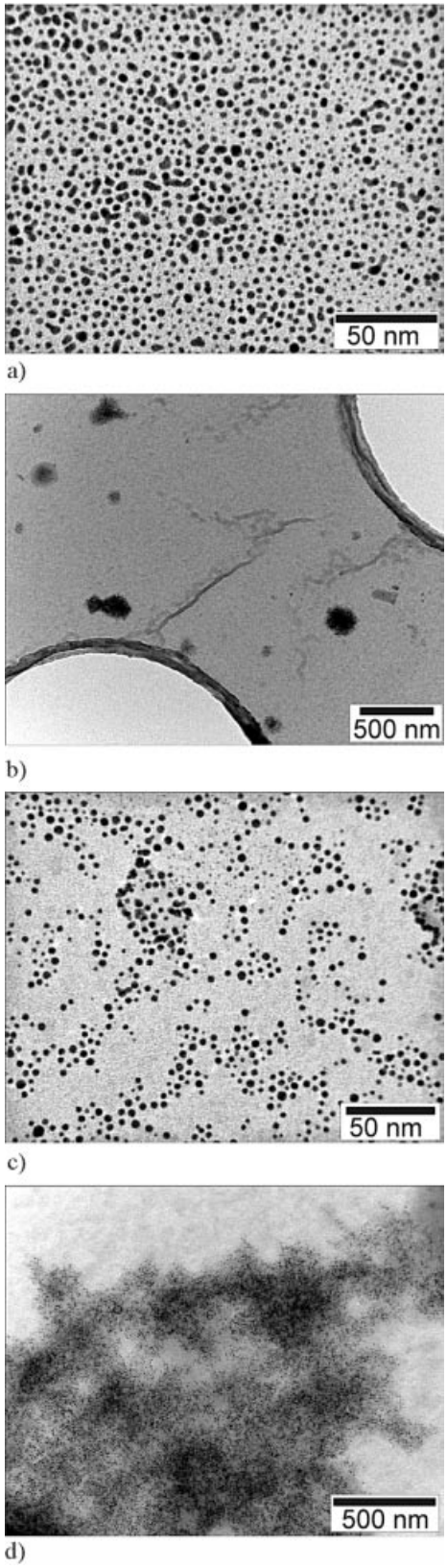

Figure 6. TEM images of aggregation events of GNPs **Au-17** and **Au-20** with Con A. a: **Au-17** in water (50 nm). b: **Au-17** incubated overnight with Con A in HEPES buffer (pH 7.4), containing 10 mM $CaCl_2$ (500 nm). c: **Au-20** in water (50 nm). d: **Au-20** incubated overnight with Con A in HEPES buffer (pH 7.4), containing 10 mM $CaCl_2$ (500 nm).

size increases with the concomitant broadening and red-shift in the particle surface plasmon band from 520 nm to a longer wavelength.[19] This results in a decrease of the measured absorbance at 520 nm, which is further augmented by the precipitation of the larger aggregates. The aggregation process is completely reversible, as judged by the clear, red/brown colored solution that was obtained after the addition of aqueous 150 mM methyl α-D-mannopyranoside (50 μL) to the precipitated aggregates. The timeframe in which this increase and subsequent decrease of absorbance at 520 nm occurs, depends on the strength of the interaction between Con A and the ligand that is displayed on the surface of the GNP. In the ligand series tested in this study, both literature[18] and our SPR data have predicted that ligand **20** would have the highest affinity for Con A. Accordingly, the decline of the UV/Vis spectrum of **Au-20** (light-green line) is the steepest of the tested compounds.

TEM Studies: The TEM micrographs of the aggregates formed during the UV/Vis experiments between either **Au-17** or **Au-20** and tetravalent Con A are shown in Figure 6. While the TEM micrographs of the aggregation between **Au-17** and Con A showed aggregates of up to 150 nm throughout the whole grid (see Figure 6, part b), the aggregates formed between **Au-20** and Con A were much larger (up to 7 μm; see Figure 6, part d).

Conclusions

A method has been established for the preparation of GNPs from free oligosaccharides. The crucial part of this method is the two-step reaction sequence for the introduction of a thiol-spacer in the free oligosaccharides. Via reductive amination, trityl-protected cysteamine was introduced into the glycan. Subsequent removal of the trityl group rendered thiol-spacer-containing oligosaccharides, in good overall yields, that can be used in the preparation of GNPs. The preparation of GNPs from the thiol-spacer-extended oligosaccharides proceeded smoothly, even with minute amounts of starting material. The prepared GNPs show complete colloidal stability, even in buffers with high salt concentrations. The prepared GNPs have been validated by their application in SPR-, UV/Vis-, and TEM-based binding assays with model lectin Con A.

The study of the proteome has identified a range of novel carbohydrate-binding proteins and, their role in biological and pathological phenomena has to be established. To achieve this, it is necessary to identify their carbohydrate ligands and, subsequently, perform interaction studies with them. Glycans, released from proteins and lipids or obtained via (partial) hydrolysis of polysaccharides, form a rich source of potential ligands for these biomolecules. GNPs, prepared from isolated glycans by using the presented method, can find application in ligand-identification processes and interaction studies with carbohydrate-binding proteins and, ultimately, help to elucidate their role in biological processes. In addition, the GNPs can find applica-

tion in the bio-medical field as inhibitors of pathological interactions and in the development of site-specific drug targeting devices.

Experimental Section

General: All chemicals were of reagent grade, and were used without further purification. The malto-oligosaccharides were purchased from Sigma–Aldrich Chemie BV (Zwijndrecht, The Netherlands) and the manno-oligosaccharides were obtained from Dextra Laboratories Ltd. (Reading, United Kingdom). $NaCNBH_3$, $NaBH_4$, and tetrachloroauric acid were purchased from Acros Organics (Geel, Belgium). *N*-Hydroxysuccinimide was purchased from Merck (NJ, USA), *N*-ethyl-*N*′-(dimethylaminopropyl)carbodiimide, ethanolamine, and Concanavalin A lectin from *Canavalia ensiformis* (Con A) from Sigma (St. Louis, USA). Cysteamine hydrochloride was supplied by Fluka (Buchs, Switzerland). C-18 Extract-Clean™ columns were purchased from Alltech (Breda, The Netherlands).

Reactions were monitored by TLC on Silica Gel 60 F_{254} (Merck); after examination under UV light, compounds were visualized by heating with 10% (v/v) methanolic H_2SO_4, orcinol (2 mg mL^{-1}) in 20% (v/v) methanolic H_2SO_4, or ninhydrin (1.5 mg mL^{-1}) in 1-butanol/water/acetic acid (38:1.75:0.25). In the work-up procedures of reaction mixtures, organic solutions were washed with appropriate amounts of the indicated aqueous solutions, then dried with $MgSO_4$, and concentrated under reduced pressure at 30–50 °C on a water bath. Column chromatography was performed on Silica Gel 60 (Merck, 0.040–0.063 mm). Purification of the larger S^2-(trityl)cysteamine-extended oligosaccharides was performed by reverse-phase HPLC on a Knauer HPLC system with a Polaris C18-A column (250 × 4.6 mm) and a linear gradient of solvent A (0.1% trifluoroacetic acid in 10% aq. acetonitrile) and solvent B (0.08% trifluoroacetic acid in 90% aq. acetonitrile) at a flow rate of 1 mL min^{-1}.

^{1}H NMR spectra were recorded at 300 K with a Bruker AC 300 (300 MHz) or a Bruker AMX 500 (500 MHz) spectrometer; δ_H values are given in ppm relative to the signal for internal acetone (δ_H = 2.22, D_2O). Two-dimensional ^{1}H-^{1}H TOCSY (mixing times 7 and 100 ms) and ^{1}H-^{13}C correlated HSQC spectra were recorded at 300 K with a Bruker AMX 500 spectrometer; δ_C values are given in ppm relative to the signal of internal acetone (δ_C = 30.9, D_2O). Surface plasmon resonance studies were carried out on a Biacore 2000 instrument, using a CM5 sensor chip and Biaevaluation software 4.1 (Pharmacia Biosensor AB, Uppsala, Sweden). Spectrophotometric measurements were performed on a Hewlett–Packard 8452A diode array instrument. All the exact masses of the oligosaccharides were measured by matrix-assisted laser desorption ionization time-of-flight mass spectrometry (MALDI-TOF MS) using a Voyager-DE Pro (Applied Biosystems) instrument in the reflector mode at a resolution of 5000 FWHM. 2,5-Dihydroxybenzoic acid in 50% aq. acetonitrile (10 mg mL^{-1}) was used as a matrix. All spectra were recorded in the positive ion-mode and a ladder of malto-oligosaccharides (G3-G13) was added as internal standard. The electrospray ionization mass spectra of compounds **12** and **18** were measured on a LCQ DecaXP ion-trap mass spectrometer equipped with an electrospray ion source (Thermo Finningan, San Jose, CA). The samples were dissolved in the mobile phase, propanol/water (1:1) to a concentration of approximately 10–30 pM μL^{-1} and introduced via a syringe pump at a flow rate of 5 μL min^{-1}. The capillary temperature was set to 225 °C and spectra were acquired in the positive ion-mode by scanning over *m*/*z* 50–2000 with a spray voltage of 4.8 kV.

***S*^{2}-(Trityl)cysteamine (1):** Cysteamine hydrochloride (200 mg, 1.73 mmol) was dissolved in dichloromethane-dimethylformamide (1:1, 10 mL). Trityl chloride (725 mg, 2.60 mmol) was added, and the solution was stirred for 2 h at room temperature. Then, the mixture was concentrated in vacuo and subsequently co-concentrated with toluene (3 × 15 mL), ethanol (3 × 15 mL), and dichloromethane (3 × 15 mL). The crude product was dissolved in dichloromethane (50 mL) and washed with saturated aq. $NaHCO_3$ (25 mL). The organic phase was dried, filtered, and concentrated in vacuo. The product was purified by flash chromatography (dichloromethane-ethyl acetate, 9:1 → dichloromethane/methanol, 4:1) to yield pure **1** (500 mg, 90%). ^{1}H NMR (300 MHz, $CDCl_3$): δ = 2.33 (t, 2 H; $H_2NCH_2CH_2STrt$), 2.59 (t, 2 H; $H_2NCH_2CH_2STrt$), 7.22 and 7.43 (2 m, 9 H and 6 H; 15 CH_{arom}).

General Procedure for the Reductive Amination of Saccharides with 1 (→ 2–11): The free saccharide (1 equiv.) and **1** (2 equiv.) were dissolved in a 5% anhydrous solution of acetic acid in dimethyl sulfoxide to a saccharide concentration of approximately 30 mM. Sodium cyanoborohydride (20 equiv.) was added, and the mixture was heated for 2 h at 65 °C. After acidification with acetic acid and dilution with water (15 mL), the mixture was loaded on a C-18 Extract-Clean™ column and unreacted saccharide was eluted with water (15 mL). Subsequent elution with methanol (15 mL) afforded a mixture of **1** and the S^2-(trityl)cysteamine-extended saccharide. The methanol fraction was concentrated in vacuo. Starting saccharides smaller than a tetrasaccharide were purified by column chromatography (dichloromethane-methanol, 6:4 → methanol → methanol/water, 1:1), while larger oligosaccharides were purified by semi-preparative RP-HPLC or solution-phase extraction procedures. The pure intermediates were characterized by high-resolution MALDI-TOF MS, and directly used in the next reaction step.

(1-Deoxy-D-glucityl)-(1→*N*)-*S*^{2}-(trityl)cysteamine (2): High-resolution MS data of $C_{27}H_{33}NO_5S$ (*M* = 483.208): M + Na found 506.189, calculated 506.198.

α-D-Glucopyranosyl-(1→4)-(1-deoxy-D-glucityl)-(1→*N*)-*S*^{2}-(trityl)-cysteamine (3): High-resolution MS data of $C_{33}H_{43}NO_{10}S$ (*M* = 645.261): M + Na found 668.253, calculated 668.251.

α-D-Glucopyranosyl-(1→4)-α-D-glucopyranosyl-(1→4)-(1-deoxy-D-glucityl)-(1→*N*)-*S*^{2}-(trityl)cysteamine (4): High-resolution MS data of $C_{39}H_{53}NO_{15}S$ (*M* = 807.313): M + Na found 830.297, calculated 830.303.

α-D-Glucopyranosyl-(1→4)-α-D-glucopyranosyl-(1→4)-α-D-glucopyranosyl-(1→4)-(1-deoxy-D-glucityl)-(1→*N*)-*S*^{2}-(trityl)cysteamine (5): High-resolution MS data of $C_{45}H_{63}NO_{20}S$ (*M* = 969.366): M + Na found 992.360, calculated 992.356.

α-D-Glucopyranosyl-(1→4)-α-D-glucopyranosyl-(1→4)-α-D-glucopyranosyl-(1→4)-α-D-glucopyranosyl-(1→4)-(1-deoxy-D-glucityl)-(1→*N*)-*S*^{2}-(trityl)cysteamine (6): High-resolution MS data of $C_{51}H_{73}NO_{25}S$ (*M* = 1131.419): M + Na found 1154.424, calculated 1154.409.

α-D-Glucopyranosyl-(1→4)-α-D-glucopyranosyl-(1→4)-α-D-glucopyranosyl-(1→4)-α-D-glucopyranosyl-(1→4)-α-D-glucopyranosyl-(1→4)-(1-deoxy-D-glucityl)-(1→*N*)-*S*^{2}-(trityl)cysteamine (7): High-resolution MS data of $C_{57}H_{83}NO_{30}S$ (*M* = 1293.472): M + Na found 1316.444, calculated 1316.462.

(1-Deoxy-D-mannityl)-(1→*N*)-*S*^{2}-(trityl)cysteamine (8): High-resolution MS data of $C_{27}H_{33}NO_5S$ (*M* = 483.208): M + Na found 506.197, calculated 506.198.

α-D-Mannopyranosyl-(1→3)-[(α-D-mannopyranosyl)-(1→6)]-(1-deoxy-D-mannityl)-(1→*N*)-*S*^{2}-(trityl)cysteamine (9): High-resolution

MS data of $C_{39}H_{53}NO_{15}S$ (M = 807.313): M + Na found 830.299, calculated 830.303.

{α-D-Mannopyranosyl-(1→6)-[(α-D-mannopyranosyl)-(1→3)]-α-D-mannopyranosyl-(1→6)}-[(α-D-mannopyranosyl)-(1→3)]-(1-deoxy-D-mannityl)-(1→*N*)-*S*^{2}-(trityl)cysteamine (10): High-resolution MS data of $C_{51}H_{73}NO_{25}S$ (M = 1131.419): M + Na found 1154.397, calculated 1154.409.

β-D-Galactopyranosyl-(1→4)-(1-deoxy-D-glucityl)-(1→*N*)-*S*^{2}-(trityl)cysteamine (11): High-resolution MS data of $C_{33}H_{43}NO_{10}S$ (M = 645.261): M + Na found 668.249, calculated 668.251.

General Procedure for the Removal of the Trityl Protecting Group (→ 12–21): The *S*^{2}-(trityl)cysteamine-extended saccharide was dissolved in a mixture of dichloromethane (1 mL) and H_2O (1 mL). Triisopropylsilane (75 μL) and trifluoroacetic acid (4 mL) were added, and the two-phase system was vigorously stirred for 15 min, then co-concentrated with toluene (3 × 20 mL) and ethanol (2 × 15 mL). The amorphous solid was dissolved in water (5 mL) and loaded on a C-18 Extract-Clean™ column. The fraction eluted with water was lyophilized to yield the cysteamine-extended saccharide.

(1-Deoxy-D-glucityl)-(1→*N*)-cysteamine (12): White powder (8.0 mg), overall yield 63%. ^{1}H NMR (500 MHz, D_2O, 2D TOCSY): δ = 4.12 (m, 1 H; H2), 3.83 (dd, $J_{2,3}$ = 5.1, $J_{3,4}$ = 2.2 Hz, 1 H; H3), 3.82 and 3.66 (2 m, each 1 H; H6a and H6b), 3.77 (m, 1 H; H5), 3.65 (dd, $J_{4,5}$ = 4.1 Hz, 1 H; H4), 3.47 (m, 2 H; DNCH_2CH$_2$SD), 3.28 (dd, $J_{1a,2}$ = 2.9, $J_{1a,1b}$ = 12.2 Hz, 1 H; H1a), 3.19 (dd, $J_{1b,2}$ = 9.6 Hz, 1 H; H1b), 3.06 (t, 2 H; DNCH$_2$CH_2SD). ^{13}C NMR (125 MHz, D_2O, HSQC): δ = 71.6 (C5), 71.5 (C4), 71.4 (C3), 69.1 (C2), 63.4 (C6), 50.4 (C1), 46.7 (NCH$_2$), 33.1 (CH$_2$S); High-resolution MS data of $C_8H_{19}NO_5S$ (M = 241.098): M + Na found 264.081, calculated 264.088.

α-D-Glucopyranosyl-(1→4)-(1-deoxy-D-glucityl)-(1→*N*)-cysteamine (13): White amorphous powder (16 mg), overall yield 61%. ^{1}H NMR (500 MHz, D_2O, 2D TOCSY): δ = 5.12 (d, $J_{1',2'}$ = 3.8 Hz, 1 H; H1′), 4.17 (m, 1 H; H2), 3.99 (m, 1 H; H5), 3.88–3.87 (m, 2 H; H3 and H4), 3.86 (m, 1 H; H5′), 3.85 (dd, $J_{5',6a'}$ = 2.2, $J_{6a',6b'}$ = 12.4 Hz, 1 H; H6a′), 3.79 (dd, $J_{5,6a}$ = 4.6, $J_{6a,6b}$ = 11.9 Hz, 1 H; H6a), 3.78 (dd, $J_{5,6b}$ = 7.0 Hz, 1 H; H6b), 3.74 (dd, $J_{2',3'}$ = 9.9, $J_{3',4'}$ = 9.5 Hz, 1 H; H3′), 3.69 (dd, $J_{5',6b'}$ = 5.5 Hz, 1 H; H6b′), 3.60 (dd, 1 H; H2′), 3.45 (m, 2 H; DNCH_2CH$_2$SD), 3.44 (dd, $J_{4',5'}$ = 9.8 Hz, 1 H; H4′), 3.26 (d, 2 H; H1a and H1b), 3.07 (t, 2 H; DNCH$_2$CH_2SD). ^{13}C NMR (125 MHz, D_2O, HSQC): δ = 101.3 (C1′), 82.2 (C4), 73.5 (C3′), 73.3 (C5′), 73.2 (C5), 72.3 (C3), 72.2 (C2′), 70.1 (C4′), 67.7 (C2), 63.0 (C6), 61.1 (C6′), 51.0 (C1), 46.6 (NCH$_2$), 33.1 (CH$_2$S); High-resolution MS data of $C_{14}H_{29}NO_{10}S$ (M = 403.151): M + Na found 426.150, calculated 426.141.

α-D-Glucopyranosyl-(1→4)-α-D-glucopyranosyl-(1→4)-(1-deoxy-D-glucityl)-(1→*N*)-cysteamine (14): White amorphous powder (9 mg), overall yield 73%. ^{1}H NMR (500 MHz, D_2O, 2D TOCSY): δ = 5.41 (d, $J_{1'',2''}$ = 3.8 Hz, 1 H; H1′′), 5.13 (d, $J_{1',2'}$ = 3.8 Hz, 1 H; H1′), 4.18 (m, 1 H; H2), 3.89–3.87 (m, 2 H; H3 and H4), 3.64 (dd, $J_{2',3'}$ = 10.1 Hz, 1 H; H2′), 3.60 (dd, $J_{2'',3''}$ = 9.9 Hz, 1 H; H2′′), 3.48 (m, 2 H; DNCH_2CH$_2$SD), 3.42 (br. t, $J_{3'',4''}$ = $J_{4'',5''}$ = 9.5 Hz, 1 H; H4′′), 3.29 (m, 2 H; H1a and H1b), 3.07 (t, 2 H; DNCH$_2$CH_2SD). ^{13}C NMR (125 MHz, D_2O, HSQC): δ = 101.1 (C1′), 100.5 (C1′′), 82.3 (C4), 72.5 (C2′′), 72.4 (C3), 72.0 (C2′), 70.1 (C4′′), 67.7 (C2), 50.8 (C1), 46.6 (NCH$_2$), 33.0 (CH$_2$S); High-resolution MS data of $C_{20}H_{40}NO_{15}S$ (M = 565.285): M + Na found 588.198, calculated 588.295.

α-D-Glucopyranosyl-(1→4)-α-D-glucopyranosyl-(1→4)-α-D-glucopyranosyl-(1→4)-(1-deoxy-D-glucityl)-(1→*N*)-cysteamine (15): White amorphous powder (4 mg), overall yield 68%. ^{1}H NMR (500 MHz, D_2O, 2D TOCSY): δ = 5.40 (d, $J_{1'',2''}$ = $J_{1''',2'''}$ = 3.9 Hz, 2 H; H1′′ and H1′′′), 5.13 (d, $J_{1',2'}$ = 3.8 Hz, 1 H; H1′), 4.16 (m, 1 H; H2), 3.88 (m, 2 H; H3 and H4), 3.45 (m, 2 H; DNCH_2CH$_2$SD), 3.42 (br. t, $J_{3''',4'''}$ = $J_{4''',5'''}$ = 9.5 Hz, 1 H; H4′′′), 3.26 (m, 2 H; H1a and H1b), 3.06 (t, 2 H; DNCH$_2$CH_2SD). ^{13}C NMR (125 MHz, D_2O, HSQC): δ = 101.1 (C1′), 100.4 (C1′′ and C1′′′), 82.3 (C4), 72.3 (C3), 70.1 (C4′′′), 67.8 (C2), 50.9 (C1), 46.7 (NCH$_2$), 33.2 (CH$_2$S); High-resolution MS data of $C_{26}H_{49}NO_{20}S$ (M = 727.257): M + Na found 750.239, calculated 750.247.

α-D-Glucopyranosyl-(1→4)-α-D-glucopyranosyl-(1→4)-α-D-glucopyranosyl-(1→4)-α-D-glucopyranosyl-(1→4)-(1-deoxy-D-glucityl)-(1→*N*)-cysteamine (16): White amorphous powder (6 mg), overall yield 81%. ^{1}H NMR (500 MHz, D_2O, 2D TOCSY): δ = 5.40 (m, 3 H; H1′′, H1′′′, and H1′′′′), 5.14 (d, $J_{1',2'}$ = 4.0 Hz, 1 H; H1′), 4.20 (m, 1 H; H2), 3.53 (m, 2 H; DNCH_2CH$_2$SD), 3.42 (br. t, $J_{3'''',4''''}$ = $J_{4'''',5''''}$ = 9.5 Hz, 1 H; H4′′′′), 3.33 (m, 2 H; H1a and H1b), 3.09 (t, 2 H; DNCH$_2$CH_2SD). ^{13}C NMR (125 MHz, D_2O, HSQC): δ = 101.0 (C1′), 100.4 (C1′′, C1′′′, and C1′′′′), 70.0 (C4′′′′), 67.4 (C2), 50.9 (C1), 46.5 (NCH$_2$), 32.5 (CH$_2$S); High-resolution MS data of $C_{32}H_{59}NO_{25}S$ (M = 889.309): M + Na found 912.291, calculated 912.299.

α-D-Glucopyranosyl-(1→4)-α-D-glucopyranosyl-(1→4)-α-D-glucopyranosyl-(1→4)-α-D-glucopyranosyl-(1→4)-α-D-glucopyranosyl-(1→4)-(1-deoxy-D-glucityl)-(1→*N*)-cysteamine (17): White amorphous powder (4 mg), overall yield 76%. ^{1}H NMR (500 MHz, D_2O, 2D TOCSY): δ = 5.39 (m, 4 H; H1′′, H1′′′, H1′′′′, and H1′′′′′), 5.12 (d, $J_{1',2'}$ = 4.0 Hz, 1 H; H1′), 4.14 (m, 1 H; H2), 3.42 (br. t, $J_{3''''',4'''''}$ = $J_{4''''',5'''''}$ = 9.5 Hz, 1 H; H4′′′′′), 3.40 (m, 2 H; DNCH_2CH$_2$SD), 3.20 (m, 2 H; H1a and H1b), 3.04 (t, 2 H; DNCH$_2$CH_2SD). ^{13}C NMR (125 MHz, D_2O, HSQC): δ = 101.1 (C1′), 100.4 (C1′′, C1′′′, C1′′′′, and C1′′′′′), 70.0 (C4′′′′′), 68.1 (C2), 51.1 (C1), 46.8 (NCH$_2$), 33.7 (CH$_2$S); High-resolution MS data of $C_{38}H_{70}NO_{30}S$ (M = 1051.363): M + Na found 1074.364, calculated 1074.353.

(1-Deoxy-D-mannityl)-(1→*N*)-cysteamine (18): Syrup (7.0 mg), overall yield 74%. ^{1}H NMR (500 MHz, D_2O, 2D TOCSY): δ = 4.03 (m, 1 H; H2), 3.85 (dd, $J_{5,6a}$ = 3.4, $J_{6a,6b}$ = 11.8 Hz, 1 H; H6a), 3.67 (dd, $J_{5,6b}$ = 5.7 Hz, 1 H; H6b), 3.52 (m, 2 H; DNCH_2CH$_2$SD), 3.49 and 3.19 (2 m, 2 H; H1a and H1b), 3.08 (t, 2 H; DNCH$_2$CH_2SD). ^{13}C NMR (125 MHz, D_2O, HSQC): δ = 67.1 (C2), 63.7 (C6), 51.2 (C1), 46.7 (NCH$_2$), 32.7 (CH$_2$S); High-resolution MS data of $C_8H_{19}NO_5S$ (M = 241.098): M + Na found 264.097, calculated 264.088.

α-D-Mannopyranosyl-(1→3)-[(α-D-mannopyranosyl)-(1→6)]-(1-deoxy-D-mannityl)-(1→*N*)-cysteamine (19): White amorphous powder (7 mg), overall yield 85%. ^{1}H NMR (500 MHz, D_2O, 2D TOCSY): δ = 5.03 (d, $J_{1'',2''}$ = 1.9 Hz, 1 H; H1′′), 4.89 (d, $J_{1',2'}$ = 1.9 Hz, 1 H; H1′), 4.16 (m, 1 H; H2), 4.04 (dd, $J_{2'',3''}$ = 3.1 Hz, 1 H; H2′′), 3.99 (dd, $J_{2',3'}$ = 3.5 Hz, 1 H; H2′), 3.56 (dd, $J_{1a,2}$ = 2.6, $J_{1a,1b}$ = 12.9 Hz, 1 H; H1a), 3.53 (m, 2 H; DNCH_2CH$_2$SD), 3.23 (dd, $J_{1b,2}$ = 10.6 Hz, 1 H; H1b), 3.08 (t, 2 H; DNCH$_2$CH_2SD). ^{13}C NMR (125 MHz, D_2O, HSQC): δ = 103.3 (C1′′), 100.7 (C1′), 70.9 (C2′′), 70.7 (C2′), 68.1 (C2), 50.4 (C1), 46.6 (NCH$_2$), 32.6 (CH$_2$S); High-resolution MS data of $C_{20}H_{40}NO_{15}S$ (M = 543.222): M + Na found 566.212, calculated 566.212.

{α-D-Mannopyranosyl-(1→6)-[(α-D-mannopyranosyl)-(1→3)]-α-D-mannopyranosyl-(1→6)}-[(α-D-mannopyranosyl)-(1→3)]-(1-deoxy-D-mannityl)-(1→*N*)-cysteamine (20): White amorphous powder (4 mg), overall yield 69%. ^{1}H NMR (500 MHz, D_2O, 2D TOCSY): δ = 5.13 (d, $J_{1'''',2''''}$ = 1.2 Hz, 1 H; H1′′′′), 5.04 (d, $J_{1''',2'''}$ = 0.6 Hz, 1 H; H1′′′), 4.91 (d, $J_{1'',2''}$ = 1.7 Hz, 1 H; H1′′), 4.86 (d,

$J_{1',2'}$ = 1.5 Hz, 1 H; H1′), 4.15 (br. t, 1 H; H2′), 4.17 (m, 1 H; H2), 4.07 (m, 1 H; H2′′′′), 4.04 (br. t, 1 H; H2′′′), 3.99 (dd, $J_{2'',3''}$ = 3.5 Hz, 1 H; H2′′), 3.56 and 3.26 (2 m, each 1 H; H1a and H1b), 3.51 (m, 2 H; DNCH_2CH$_2$SD), 3.07 (t, 2 H; DNCH$_2$CH_2SD). ^{13}C NMR (125 MHz, D_2O, HSQC): δ = 103.2 (C1′′′), 103.1 (C1′′′′), 100.8 (C1′), 100.1 (C1′′), 70.7 (C2′′′ and C2′′′′), 70.6 (C2′′), 70.4 (C2′), 68.1 (C2), 50.6 (C1), 46.5 (NCH_2), 32.6 (CH_2S); High-resolution MS data of $C_{32}H_{59}NO_{25}S$ (M, 889.310): M + Na found 912.311, calculated 912.300.

β-D-Galactopyranosyl-(1→4)-(1-deoxy-D-glucityl)-(1→*N*)-cysteamine (21): Slightly yellow powder (5 mg), overall yield 67%. ^{1}H NMR (500 MHz, D_2O, 2D TOCSY): δ = 4.53 (d, $J_{1',2'}$ = 7.8 Hz, 1 H; H1′), 4.23 (m, 1 H; H2), 3.93 (br. d, $J_{3',4'}$ = 3.5, $J_{4',5'} < 1$ Hz, 1 H; H4′), 3.80 (dd, $J_{2,3}$ = 2.0, $J_{3,4}$ = 5.1 Hz, 1 H; H3), 3.67 (dd, $J_{2',3'}$ = 9.9 Hz, 1 H; H3′), 3.55 (dd, 1 H; H2′), 3.48 (m, 2 H; DNCH_2CH$_2$SD), 3.40 (dd, $J_{1a,2}$ = 4.6, $J_{1a,1b}$ = 12.7 Hz, 1 H; H1a), 3.18 (dd, $J_{1b,2}$ = 10.1 Hz, 1 H; H1b), 3.07 (t, 2 H; DNCH$_2$CH_2SD). ^{13}C NMR (125 MHz, D_2O, HSQC): δ = 103.6 (C1′), 75.9 (C3), 73.1 (C3′), 71.7 (C2′), 71.6 (C4′), 68.4 (C2), 50.4 (C1), 46.7 (NCH_2), 32.9 (CH_2S); High-resolution MS data of $C_{14}H_{29}NO_{10}S$ (M = 403.151): M + Na found 426.138, calculated 426.141.

General Procedure for the Preparation of GNPs Au-13 to Au-17 and Au-19 to Au-21: A solution of a cysteamine-extended saccharide (**12** to **21**) in water (10 mM, 1 equiv.) was added to a solution of tetrachloroauric acid in water (25 mM, 1 equiv.). Then, aq. $NaBH_4$ (1 M, 40 equiv.) was slowly added under vigorous stirring, and the obtained red/brown solution was stirred for 2 h at room temperature. After neutralization with 30% aq. acetic acid, the solution was diluted with water (10 mL), loaded on a 30 kDa Nalgene centrifugal filter, and filtered. The residue was several times redissolved in water and filtered (5 × 5 mL). After lyophilization from water, the GNPs **Au-13** to **Au-17** and **Au-19** to **Au-21** were obtained as brown, amorphous powders. The GNPs were characterized by 500 MHz ^{1}H NMR spectroscopy in D_2O, monosaccharide analysis, and transmission electron microscopy (TEM).

Preparation of GNPs Au-14a and Au14b: The procedure is the same as described above, only 2 equiv. or 0.33 equiv. of **14**, as compared to tetrachloroauric acid, were added for the preparation of GNPs **Au-14a** and **Au-14b**, respectively.

Preparation of GNPs Au-17a: To a solution of **17** (0.1 mg, 95 nmol) in water (50 μL) was added 12 μL aq. tetrachloroauric acid (25 nM, 285 nmol). Then, 120 μL aq. $NaBH_4$ (0.1 M, 1.14 μmol) was slowly added under ultrasonic stirring. The obtained red/brown solution was sonicated for 5 min, then left for 2 h at room temperature. After neutralization with 30% aq. acetic acid, the solution was diluted with water (1 mL), loaded on a 30 kDa eppendorf centrifugal filter, and filtered. The residue was several times redissolved in water and filtered (5 × 1 mL). After lyophilization from water, the GNPs **Au-17a** were obtained as a brown, amorphous powder. The GNPs were characterized by 500 MHz ^{1}H NMR spectroscopy in D_2O and transmission electron microscopy (TEM).

Monosaccharide Analysis: After adding internal standard (mannitol), the GNP samples were subjected to methanolysis (1 M methanolic HCl, 24 h, 85 °C), followed by trimethylsilylation. The trimethylsilylated methyl glycosides were analyzed by GLC on an EC-1 capillary column (30 m × 0.32 mm, Alltech) using a Chrompack CP 9002 gas chromatograph (temperature program, 140–240 °C at 4 °C min^{-1}). The identification of the monosaccharide derivatives was confirmed by gas chromatography/mass spectrometry on a Fisons Instruments GC 8060/MD 800 system (Interscience) equipped with an AT-1 capillary column (30 m × 0.25 mm, Alltech), using the same temperature program.[16]

SPR Binding Assays: CM5 sensor surfaces were equilibrated with HEPES buffer (10 mM HEPES pH 7.4, 0.15 M NaCl), then activated with a 14-min pulse of a 1:1 mixture (v/v) of 0.1 M *N*-hydroxysuccinimide and 0.1 M *N*-ethyl-*N*′-(dimethylaminopropyl)carbodiimide, at 25 °C and a flow rate of 5 μL min^{-1}. Ethanolamine hydrochloride was immobilized on channel 1 via an injection of 7 min (1.0 M, pH 8.5; ≈ 300 RU) to measure the level of non-specific binding and to serve as blank channel for mathematical data treatment. Con A was attached to channel 2 via an injection of 1 min (50 μg mL^{-1} in 10 mM sodium acetate buffer, pH 4.8; ≈ 400 RU) and to channel 3 via an injection of 7 min (100 μg mL^{-1} in 10 mM sodium acetate buffer, pH 4.8; ≈ 7.000 RU); remaining *N*-hydroxysuccinimide esters were blocked by a 7-min pulse of 1.0 M ethanolamine hydrochloride, pH 8.5.

GNPs **Au-13** to **Au-17** and **Au-19** to **Au-21** (100 μg mL^{-1}, and dilutions thereof) in HEPES buffer, containing 10 mM $CaCl_2$, were flowed across the sensor chip surfaces for 3 min at a flow rate of 15 μL min^{-1}, and were allowed to dissociate for 5 min. To restore the response level to zero after **Au-13** to **Au-17** injections, 150 mM methyl α-D-mannopyranoside and 3 M NaCl were sequentially injected for 5 min. After an **Au-19** injection, the sensor chip surface was regenerated by sequentially injecting 600 mM methyl α-D-mannopyranoside and 3 M NaCl for 5 min. Multiple (6x), 10 min long sequential injections of 1.2 M methyl α-D-mannopyranoside containing 50 mM EDTA and 1 M NaCl were required to regenerate the sensor chip surface after **Au-20** was injected.

Spectrophotometric Aggregation Assay: A solution (500 μL) of GNPs **Au-13** to **Au-17** and **Au-19** to **Au-21** (100 μg mL^{-1}) in HEPES buffer (pH 7.4), containing 10 mM $CaCl_2$, and 50 μL of Con A (1 mg mL^{-1}), dissolved in the same HEPES buffer, were mixed in a quartz cuvet. Spectrophotometric analysis was performed by measuring, every 5 min for 6 h, the absorbance at 520 nm on a Hewlett–Packard 8452A diode array spectrophotometer.

Transmission Electron Microscopy: Prior to the examination of the aggregates formed between **Au-17** and Con A, and **Au-20** and Con A (see spectrophotometric aggregation assay in experimental section), the HEPES buffer, containing 10 mM $CaCl_2$, was removed by centrifugal filtration through a 30 kDa eppendorf centrifugal filter and replaced by water. Examinations were performed with a Philips Tecnai12 microscope at 120 kV accelerating voltage. Aliquots (1 μL) of GNPs **Au-17** and **Au-20** (0.1 mg mL^{-1}), before and after aggregation, were placed onto copper grids coated with a carbon film (QUANTIFOIL on 200 square mesh copper grid, hole shape R 2/2). The grids were left to dry at room temperature for several hours. The particle size distribution of the GNPs was automatically determined from several micrographs of the same sample, using analySIS® 3.2 (Soft Imaging System GmbH).

Acknowledgments

The financial support of the Academic Biomedical Center, Utrecht University (Expertise Center for Carbohydrate Analysis and Synthesis) is highly acknowledged (J. P. K., K. M. H. and A. C. S.). P. Rohfritsch is kindly acknowledged for measuring the ES-MS spectra. J. P. Meeldijk is kindly acknowledged for his assistance with the TEM measurements.

[1] N. Perrimon, M. Bernfield, *Nature* **2000**, *404*, 725–728.
[2] P. R. Crocker, T. Feizi, *Curr. Opin. Struct. Biol.* **1996**, *6*, 679–691.
[3] Y. C. Lee, R. T. Lee, *Acc. Chem. Res.* **1995**, *28*, 321–327.

[4] H. Lis, N. Sharon, *Chem. Rev.* **1998**, *98*, 637–674.
[5] Y. C. Lee, *FASEB J.* **1993**, *6*, 3193–3200.
[6] B. Benaissa-Trouw, D. J. Lefeber, J. P. Kamerling, J. F. G. Vliegenthart, H. Snippe, K. Kraaijeveld, *Inf. Imm.* **2001**, *69*, 4698–4701.
[7] S. Andre, P. J. Ortega, M. A. Perez, R. Roy, H.-J. Gabius, *Glycobiology* **1999**, *9*, 1253–1261.
[8] K. Matsuura, H. Kitakouji, N. Sawada, H. Ishida, M. Kiso, K. Kitajima, K. Kobayashi, *J. Am. Chem. Soc.* **2000**, *122*, 7406–7407.
[9] J. M. de la Fuente, A. G. Barrientos, T. C. Rojas, J. Roja, A. Fernández, S. Penadés, *Angew. Chem. Int. Ed.* **2001**, *40*, 2257–2261.
[10] A. Carvalho de Souza, K. M. Halkes, J. D. Meeldijk, A. J. Verkleij, J. F. G. Vliegenthart, J. P. Kamerling, *Eur. J. Org. Chem.* **2004**, 4323–4339.
[11] H. Otsuka, Y. Akiyama, Y. Nagasaki, K. Kataoka, *J. Am. Chem. Soc.* **2001**, *123*, 8226–8230.
[12] C.-C. Lin, Y.-C. Yeh, C.-Y. Yang, C.-L. Chen, G.-F. Chen, C.-C. Chen, Y.-C. Wu, *J. Am. Chem. Soc.* **2002**, *124*, 3508–3509.
[13] A. G. Barrientos, J. M. de la Fuente, T. C. Rojas, A. Fernández, S. Penadés, *Chem. Eur. J.* **2003**, *9*, 1909–1921.
[14] A. Carvalho de Souza, K. M. Halkes, J. D. Meeldijk, A. J. Verkleij, J. F. G. Vliegenthart, J. P. Kamerling, *ChemBioChem* **2005**, *6*, 828–831.
[15] M. Brust, M. Walker, D. Berthell, D. J. Schiffrin, R. Whyman, *J. Chem. Soc. Chem. Commun.* **1994**, 801–802.
[16] J. P. Kamerling, J. F. G. Vliegenthart, in *Clinical Biochemistry – Principles, Methods, Applications 1. Mass Spectrometry* (Ed.: A. M. Lawson), Walter de Gruyter, Berlin, **1989**, 176–263.
[17] M. J. Hostetler, J. E. Wingate, C.-J. Zhong, J. E. Harris, R. W. Vachet, M. R. Clark, J. D. Londono, S. J. Green, J. J. Stokes, G. D. Wignall, G. L. Glish, M. D. Porter, N. D. Evans, R. W. Murray, *Langmuir* **1998**, *14*, 17–30.
[18] H. Kaku, I. J. Goldstein, *Carbohydr. Res.* **1992**, *229*, 337–346.
[19] G. Mie, *Ann. Phys.* **1908**, *25*, 377.
[20] D. C. Hone, A. H. Haines, D. A. Russell, *Langmuir* **2003**, *19*, 7141–7144.

Received: April 12, 2005
Published Online: July 12, 2005

